

Asymptotically stable Particle-in-Cell methods for the magnetized Vlasov–Poisson equations in orthogonal curvilinear coordinates

Anjiao Gu¹ and Yajuan Sun^{2,3}

¹Department of mathematics, Institute of Natural Sciences and MOE-LSC. Shanghai Jiao Tong University, Shanghai, 200240, China

²LSEC, ICMSEC, Academy of Mathematics and Systems Science, Chinese Academy of Sciences, Beijing, 100190, China

³School of Mathematical Sciences, University of Chinese Academy of Sciences, Beijing, 100190, China

July 15, 2024

Abstract

In high-temperature plasma physics, a strong magnetic field is usually imposed to confine the large amount of charged particles. Therefore, for studying the classical mathematical models of the physical problems it needs to consider the effect of external magnetic fields. One of the important model equations in plasma is the Vlasov–Poisson equation with an external magnetic field. This equation usually has multi-scale characteristics and rich physical properties, thus it is very important and meaningful to construct numerical methods that can maintain the physical properties inherited by the original systems over long time. In this paper, we have presented the construction and theory of numerical methods for physical problems in general orthogonal curvilinear coordinates and proved that a Poisson-bracket structure can still be obtained after applying the appropriate finite element discretizations. However, the Hamiltonian systems in the new coordinate systems generally cannot be decomposed into subsystems that can be solved exactly, thus in this paper we propose a semi-implicit numerical method. This method has been applied to solve the problem under strong magnetic fields and its asymptotic stability has been analyzed.

Keywords: Magnetized Vlasov–Poisson equation, Curvilinear coordinate, Particle method, Asymptotically stable

1 Introduction

Physical problem in plasma is a multi-particle system of charged particles coupled with electromagnetic fields. In general, it is considered to be a classical system, i.e.,

it does not take relativistic effects into account. Charged particles are the basic units of the plasma. If the concern is with the kinetic behavior of individual particles in an electromagnetic field, this can be examined through Newton's equations. Whereas, when studying the macroscopic motion of plasma, if its density is large and particle collisions are frequent, it can be considered to be approximated as an electrically conducting fluid. The theory that explores the laws of motion of an electrically conducting fluid in an electromagnetic field is also known as magneto-fluid mechanics. If the physical process has to take into account the velocity distribution of each particle, it is necessary to use kinetic theory to describe the plasma. The Vlasov equation is an important model for this purpose.

The properties of physical problem in plasma are more complex than those of ordinary fluids and have a wide range of applications. Therefore exploring and characterizing their kinetic behavior is a challenging and important research direction. Although the design of numerical algorithms for the Vlasov equation has attracted a lot of attention since the 1960s, structure-preserving algorithms based on its geometric properties have only recently been investigated and rapidly become a hot topic, see [13, 30, 39] and references therein. This is because structure-preserving algorithms are uniquely suited for simulations that maintain conserved quantities and long-term kinetic behavior [8, 9], which fits the need to study the kinetic behavior of charged particles. Vlasov systems have a number of geometric structural properties, so it is therefore natural to consider these properties in the discretization process. For example, the Vlasov–Maxwell equation has variational [38, 7, 36] and Hamiltonian structure [28, 25, 27], and also a series of conserved quantities.

Currently, most of the work on geometric algorithms for the Vlasov equation has been done in the Cartesian coordinate system [5, 40, 37, 21, 23, 2, 24]. However, it's common to characterize the problem in terms of its configuration in magnetic confinement fusion, like Tokamak, which is a toroidal device. In this case, the physical phenomena of interest can be examined more easily by using the corresponding other coordinates. This motivates us to extend some of the geometric descriptions and numerical frameworks developed in Cartesian coordinates to the general curvilinear coordinate case. Unfortunately, structure-preserving algorithms do not generally follow directly from Cartesian coordinates to curvilinear coordinates, so this makes it difficult for us to construct numerical algorithms. In the framework of curvilinear coordinates, particle methods [22, 1] have been developed in the literature, and more recently the literature has extended the structure-preserving algorithms for the Vlasov–Maxwell equation [33, 35]. In this paper, we discuss structure-preserving algorithms for the Vlasov–Poisson equation in curvilinear coordinates. By proving that the solution of the variational problem in orthogonal coordinates still exists and unique, we can still use the finite element method in space. In the case where the Hamiltonian splitting algorithm is no longer applicable, we develop an asymptotically stable semi-implicit method which studied in [11, 12].

The outline of the paper is as follows. In section 2, we introduce magnetized Vlasov–Poisson equation. Then in section 3 we present the equation in orthogonal curvilinear coordinates and construct spatial discretization which makes semi-discrete system maintaining a Hamiltonian structure. Furthermore, we discuss time discretizations and prove the asymptotically stable property for the semi-implicit methods in Section 4. In Section 5, we display the numerical results. Finally, we conclude this paper.

2 The magnetized Vlasov–Poisson equation

For the research of magnetic confinement fusion, it is natural and necessary to introduce the effect of an external magnetic field. We consider a plasma consisting of a large number of charged particles while its distribution is described by the Vlasov equation. The self-consistent electric field is expressed by the potential and the potential satisfies the Poisson equation. Specifically, the model for studying the long time behavior of the plasma can be expressed as the following magnetized Vlasov–Poisson equation,

$$\begin{aligned} \varepsilon \frac{\partial f}{\partial t} + v \cdot \frac{\partial f}{\partial x} + (\mathbf{E} + \frac{1}{\varepsilon} v \times \mathbf{B}) \cdot \frac{\partial f}{\partial v} &= 0, \\ \mathbf{E} &= -\nabla_x \phi, \quad \nabla_x \cdot \mathbf{B} = 0, \\ -\Delta \phi &= \rho(x, t) - \rho_0, \\ \rho &= \int_{\mathbb{R}^3} f dv, \end{aligned} \tag{1}$$

where f is the distribution function of the particle, $x, v \in \mathbb{R}^3, t \in \mathbb{R}_+$ denotes position, velocity and time in turn. $\mathbf{E}, \mathbf{B} \in \mathbb{R}^3$ are the self-consistent electric field and external magnetic field respectively. Here, ε is not only a parameter which is inversely proportional to the strength of the magnetic field, but also a time rescaling to simulate long time behavior. The initial distribution satisfies $f(x, v, 0) = f_0(x, v)$. Furthermore, function ρ denotes the density of the charge, and the ions are assumed to be homogeneous and their density is ρ_0 . In [14], we have presented the following Poisson bracket of (1)

$$\begin{aligned} \{\{\mathcal{F}, \mathcal{G}\}\}(f) &= \int_{\mathbb{R}^3} \int_{\mathbb{R}^3} f \left\{ \frac{\delta \mathcal{F}}{\delta f}, \frac{\delta \mathcal{G}}{\delta f} \right\}_{xv} dx dv \\ &+ \frac{1}{\varepsilon} \int_{\mathbb{R}^3} \int_{\mathbb{R}^3} f \mathbf{B} \cdot \left(\frac{\partial}{\partial v} \frac{\delta \mathcal{F}}{\delta f} \times \frac{\partial}{\partial v} \frac{\delta \mathcal{G}}{\delta f} \right) dx dv, \end{aligned} \tag{2}$$

where \mathcal{F} and \mathcal{G} are two functionals of f , $\frac{\delta \mathcal{F}}{\delta f}$ is the variational derivative. In (2), the operator $\{\cdot, \cdot\}_{xv}$ is the canonical Poisson bracket which for two given functions $m(x, v)$ and $n(x, v)$, that is

$$\{m, n\}_{xv} = \frac{\partial m}{\partial x} \cdot \frac{\partial n}{\partial v} - \frac{\partial m}{\partial v} \cdot \frac{\partial n}{\partial x}.$$

With the bracket (2), we consider the following Poisson system

$$\varepsilon \frac{d\mathcal{F}}{dt} = \{\{\mathcal{F}, \mathcal{H}\}\}, \tag{3}$$

where \mathcal{F} is any functional of f , and \mathcal{H} is the Hamiltonian functional which is also the global energy of the system,

$$\begin{aligned} \mathcal{H}[f] &= \frac{1}{2} \int_{\mathbb{R}^3} \int_{\mathbb{R}^3} |v|^2 f dx dv + \frac{1}{2} \int_{\mathbb{R}^3} |\mathbf{E}|^2 dx \\ &= \frac{1}{2} \int_{\mathbb{R}^3} \int_{\mathbb{R}^3} |v|^2 f dx dv + \frac{1}{2} \int_{\mathbb{R}^3} \int_{\mathbb{R}^3} \phi f dx dv - \frac{1}{2} \rho_0 \int_{\mathbb{R}^3} \phi dx. \end{aligned} \tag{4}$$

In fact, by setting $\mathcal{F}[f] = \int_{\mathbb{R}^3} \int_{\mathbb{R}^3} f(\tilde{x}, \tilde{v}, t) \delta(x - \tilde{x}) \delta(v - \tilde{v}) d\tilde{x} d\tilde{v}$, and defining the local energy $h(x, v) = \frac{\delta \mathcal{H}}{\delta f}(x, v) = |v|^2/2 + \phi(x)$, it follows from (3) that

$$\varepsilon \frac{\partial f}{\partial t} = -\{f, h\}_{xv} - \frac{1}{\varepsilon} \mathbf{B} \cdot \left(\frac{\partial f}{\partial v} \times \frac{\partial h}{\partial v} \right)$$

which recovers the Vlasov equation (1). This implies that the magnetized Vlasov–Poisson equation can be written in a Poisson system.

As an approximate model of the Vlasov–Maxwell equations, the Vlasov–Poisson system also has many important conservation properties. Through Poisson bracket (2) and expression (3), its conservation properties can be described by the following proposition.

Proposition 2.1. *In the Vlasov–Poisson system (1), if the potential ϕ has a zero boundary or periodic boundary, it has the following conserved quantities:*

(1) **Conservation of energy:** *The total energy (4) is an invariant of the system.*

(2) **Conservation of momentum:** *the total momentum $\mathcal{P} = \int_{\mathbb{R}^3 \times \mathbb{R}^3} v f dx dv$ is also an invariant when $\mathbf{B} = 0$.*

(3) **Casimir functional:** *any form $\mathcal{C}[f] = \int_{\mathbb{R}^3 \times \mathbb{R}^3} C(f) dx dv$ is an invariant when $\mathbf{B} = 0$, and is also called a Casimir functional [29] with respect to the Poisson bracket (2).*

3 Curvilinear coordinates

Different equations are expressed in different forms when using different coordinate systems, and they are often not expressed in the simplest form in the Cartesian coordinate. For example, the spherical equation $x_1^2 + x_2^2 + x_3^2 = R^2$ can be written as $r = R$ in spherical coordinate (r, φ, θ) . Therefore, studying equations in curvilinear coordinates has broad significance. Some frequently used vector fields in orthogonal curvilinear coordinates are given in the appendix A.

3.1 Transformation

We consider the bijective coordinate transformation from the space $\tilde{\Omega}_y$ to Ω_x . The transformation is denoted by

$$F : \tilde{\Omega}_y \rightarrow \Omega_x \subset \mathbb{R}^3, \quad F(y) = x.$$

The Jacobi matrix is denoted by $D_F(y)$, and its elements are

$$(D_F(y))_{ij} = \frac{\partial x_i}{\partial y_j},$$

the corresponding Jacobian is $J(y) = \det(D_F(y))$. Moreover, we assume that the new coordinates are orthogonal and $J(y) > 0$. If $J(y) < 0$, we only need to apply the permutation of y_i and y_j once so that the new Jacobian $J(y') > 0$ about the transformation y' . Also, $J(y) \neq 0$ due to the orthogonality. Then we can denote $D_F(y)^{-T}$ as $N(y)$. The curvilinear coordinates to the differential forms have been introduced as the following proposition.

Proposition 3.1. For a scalar differential 0-form $g \in H^1(\Omega_x)$, we can define $\tilde{g} \in H^1(\tilde{\Omega}_y)$ as

$$\tilde{g}(y) = g(x).$$

For a vector differential 1-form $\mathbf{E} \in H(\text{curl}, \Omega_x)$, it has $\tilde{\mathbf{E}} \in H(\text{curl}, \tilde{\Omega}_y)$ connected by

$$\mathbf{E}(x) = N(y)\tilde{\mathbf{E}}(y).$$

For a vector differential 2-form $\mathbf{B} \in H(\text{div}, \Omega_x)$, we have $\tilde{\mathbf{B}} \in H(\text{div}, \tilde{\Omega}_y)$ through

$$\mathbf{B}(x) = \frac{D_F(y)}{J(y)}\tilde{\mathbf{B}}(y).$$

For a scalar differential 3-form $h \in L^2(\Omega_x)$, we can obtain $\tilde{h} \in L^2(\tilde{\Omega}_y)$ via

$$h(x) = \frac{1}{J(y)}\tilde{h}(y).$$

The proof can be obtained directly from Appendix A or literature [34]. Then we can have $\nabla_x \cdot \mathbf{B} = \frac{1}{J(y)}\nabla_y \cdot \tilde{\mathbf{B}}$ and $\nabla_x = N(y)\nabla_y$. According to Proposition 3.1, we can transform the Vlasov–Poisson system (1) to

$$\begin{aligned} \varepsilon \frac{\partial \tilde{f}}{\partial t} + N(y)^T v \cdot \frac{\partial \tilde{f}}{\partial y} + N(y)(\tilde{\mathbf{E}} + \frac{1}{\varepsilon}(N(y)^T v) \times \tilde{\mathbf{B}}) \cdot \frac{\partial \tilde{f}}{\partial v} &= 0, \\ \nabla_y \cdot \tilde{\mathbf{B}} &= 0, \quad -N(y)\nabla_y \cdot N(y)\nabla_y \tilde{\phi} = \int_{\mathbb{R}^3} \tilde{f} dv - \rho_0. \end{aligned} \quad (5)$$

Remark. It is worth mentioning that \tilde{f} is no longer conserved, but $J\tilde{f}$ is. In other words,

$$\varepsilon \frac{\partial J\tilde{f}}{\partial t} + \nabla_y \cdot (N^T v J\tilde{f}) + \nabla_v \cdot (N(\tilde{\mathbf{E}} + \frac{1}{\varepsilon}(N^T v) \times \tilde{\mathbf{B}})J\tilde{f}) = 0.$$

Some corresponding conservative methods can be found in [3, 20].

We use Particle-in-cell method to obtain a discrete distribution function which reads

$$f_h(x, v, t) = \sum_{s=1}^{N_p} \alpha_s \delta(x - X_s(t)) \delta(v - V_s(t)).$$

After the transformation, the distribution function becomes to

$$\tilde{f}_h(y, v, t) = \sum_{s=1}^{N_p} \alpha_s \frac{\delta(y - Y_s(t))}{J(y)} \delta(v - V_s(t))$$

due to the Dirac function δ . To generate particles more conveniently, the following equivalent form can be used

$$J(y)\tilde{f}_h(y, v, t) = \sum_{s=1}^{N_p} \alpha_s \delta(y - Y_s(t)) \delta(v - V_s(t)).$$

Thus Vlasov equation in (5) transforms into the following particle equation

$$\begin{aligned} \varepsilon \dot{Y}_s &= N(Y_s)^T V_s, \\ \varepsilon \dot{V}_s &= N(Y_s)\tilde{\mathbf{E}}(Y_s) + \frac{1}{\varepsilon}N(Y_s)\hat{\tilde{\mathbf{B}}}(Y_s)N(Y_s)^T V_s, \quad s = 1, 2, \dots, N_p. \end{aligned} \quad (6)$$

3.2 Spatial discretization and Hamiltonian structure

In [14], we discretized the space with finite element method to ensure that $\phi_h \in H_0^1(\Omega_x)$, thus making the semi-discrete system Hamiltonian. We follow this to the curvilinear coordinate case, i.e., $\tilde{\phi}_h \in H_0^1(\tilde{\Omega}_y)$.

The first step for finite element discretization is to determine the variational problem. Then the corresponding bilinear form need to obey the conditions of Lax-Milgram theorem. That is, it should be bounded and coercive. The following theorem ensures this.

Theorem 3.1. *The bilinear form $a'(u, v) = -\int_{\tilde{\Omega}} (N(y)\nabla_y \cdot N(y)\nabla_y u)vJ(y)dy$ is bounded and coercive.*

Proof. By noticing that

$$N(y)\nabla_y \cdot N(y)\nabla_y u = \frac{1}{H_1 H_2 H_3} \sum_{ijk} \frac{\partial}{\partial y_i} \left(\frac{H_j H_k}{H_i} \frac{\partial u}{\partial y_i} \right)$$

where H_1, H_2, H_3 are Lamé coefficients, it's obvious since $H_i > 0$ and $H_1 H_2 H_3 = J(y)$. \square

We assume a finite dimensional space \tilde{V}_h is the subspace of $H_0^1(\tilde{\Omega}_y)$ and $\{W_j(y)\}_{j=1}^N$ are piecewise polynomial basis functions of it. The discrete potential function $\tilde{\phi}_h \in \tilde{V}_h$ can be expressed as

$$\tilde{\phi}_h(y, t) = \sum_{j=1}^N \tilde{\phi}_j(t) W_j(y). \quad (7)$$

Substituting (7) into the particle equation (6), then we have

$$\begin{aligned} \varepsilon \dot{Y}_s &= N(Y_s)^T V_s, \\ \varepsilon \dot{V}_s &= -N(Y_s) \sum_{j=1}^N \tilde{\phi}_j \nabla W_j(Y_s) + \frac{1}{\varepsilon} N(Y_s) \hat{\mathbf{B}}(Y_s) N(Y_s)^T V_s, \quad s = 1, 2, \dots, N_p. \end{aligned} \quad (8)$$

We can represent the equation with the following discrete Poisson bracket (8). For any functions F and G on (Y, V) , define the bracket

$$\begin{aligned} \{F, G\}(Y, V) &= \sum_{s=1}^{N_p} \frac{1}{\alpha_s} \left(N(Y_s) \frac{\partial F}{\partial Y_s} \cdot \frac{\partial G}{\partial V_s} - N(Y_s) \frac{\partial G}{\partial Y_s} \cdot \frac{\partial F}{\partial V_s} \right) \\ &+ \sum_{s=1}^{N_p} \frac{1}{\alpha_s} \frac{D_F(Y_s)}{\varepsilon J(Y_s)} \hat{\mathbf{B}}(Y_s) \cdot \left(\frac{\partial F}{\partial V_s} \times \frac{\partial G}{\partial V_s} \right). \end{aligned} \quad (9)$$

and discrete Hamiltonian function

$$H(Y, V) = \frac{1}{2} \sum_{s=1}^{N_p} \alpha_s |V_s|^2 + \frac{1}{2} \sum_{j=1}^N \sum_{k=1}^N \phi_j(Y) \phi_k(Y) a'(W_j, W_k). \quad (10)$$

By means of discrete bracket (9) and discrete Hamiltonian (10), the semi-discrete system (8) can be written as

$$\varepsilon \dot{Y}_s = \{Y_s, H\}, \quad \varepsilon \dot{V}_s = \{V_s, H\}.$$

In the following we express the semi-discrete system (8) in matrix form. First we introduce the following notations:

$$\begin{aligned}\tilde{\Phi}(Y) &= (\tilde{\phi}_1, \tilde{\phi}_2, \dots, \tilde{\phi}_N)^T(Y) \in \mathbb{R}^N, \quad \mathbb{M} \in \mathbb{R}^{N \times N}, \quad \mathbb{M}_{jk} = a'(W_j, W_k), \\ \mathbb{G}(Y) &= \begin{pmatrix} \nabla W_1(Y_1) & \nabla W_2(Y_1) & \cdots & \nabla W_N(Y_1) \\ \nabla W_1(Y_2) & \nabla W_2(Y_2) & \cdots & \nabla W_N(Y_2) \\ \cdots & \cdots & \cdots & \cdots \\ \nabla W_1(Y_{N_p}) & \nabla W_2(Y_{N_p}) & \cdots & \nabla W_N(Y_{N_p}) \end{pmatrix} \in \mathbb{R}^{(3N_p) \times N}, \\ \tilde{\mathbb{B}}(Y) &= \text{diag}(\hat{\mathbb{B}}(Y_1), \hat{\mathbb{B}}(Y_2), \dots, \hat{\mathbb{B}}(Y_{N_p})) \in \mathbb{R}^{(3N_p) \times (3N_p)}, \\ \mathbb{N} &= \text{diag}(N(Y_1), N(Y_2), \dots, N(Y_{N_p})) \in \mathbb{R}^{(3N_p) \times (3N_p)}.\end{aligned}$$

Define the diagonal weight matrix $\Omega = \text{diag}(\alpha_1, \alpha_2, \dots, \alpha_{N_p}) \in \mathbb{R}^{N_p \times N_p}$ and 3-dimensional identity matrix I . Further we note that

$$\mathbb{W} = \Omega \otimes I \in \mathbb{R}^{(3N_p) \times (3N_p)}.$$

Thus, the discrete Poisson bracket (9) can be rewritten in the following matrix form

$$\{F, G\}(Z) = \frac{\partial F^T}{\partial Z} \mathbb{K}(Y) \frac{\partial G}{\partial Z}, \quad (11)$$

with $Z = (Y^T, V^T)^T$, and

$$\mathbb{K}(Y) = \begin{pmatrix} 0 & \mathbb{W}^{-1} \mathbb{N}(Y)^T \\ -\mathbb{W}^{-1} \mathbb{N}(Y) & \frac{1}{\varepsilon} \mathbb{W}^{-1} \mathbb{N}(Y) \tilde{\mathbb{B}}(Y) \mathbb{N}(Y)^T \end{pmatrix} \quad (12)$$

is the Poisson matrix corresponding to the bracket (9). After using the above notations, the discrete Hamiltonian (10) can be written as

$$H(Y, V) = \frac{1}{2} V^T \mathbb{W} V + \frac{1}{2} \tilde{\Phi}(Y)^T \mathbb{M} \tilde{\Phi}(Y). \quad (13)$$

The corresponding system (8) can be rewritten in terms of the Poisson matrix $\mathbb{K}(X)$ as

$$\begin{aligned}\varepsilon \dot{Y} &= \mathbb{N}(Y)^T V, \\ \varepsilon \dot{V} &= \mathbb{N}(Y) \mathbb{G}(Y) \tilde{\Phi}(Y) + \frac{1}{\varepsilon} \mathbb{N}(Y) \tilde{\mathbb{B}}(Y) \mathbb{N}(Y)^T V.\end{aligned} \quad (14)$$

Theorem 3.2. *Discrete bracket (11) with respect to system (14) is a Poisson bracket.*

Proof. According to proposition B.1, we need to verify the matrix (12) satisfies

$$\sum_{l=1}^{6N_p} \left(\frac{\partial \mathbb{K}_{ij}}{\partial Z^l} \mathbb{K}_{lk} + \frac{\partial \mathbb{K}_{jk}}{\partial Z^l} \mathbb{K}_{li} + \frac{\partial \mathbb{K}_{ki}}{\partial Z^l} \mathbb{K}_{lj} \right) = 0,$$

for all indexes $i, j, k \in \{1, \dots, 6N_p\}$ and $Z = (Y, V)$.

Since the matrix (12) depends on Y , we only need to consider the case of $l \in \{1, \dots, 3N_p\}$. That is,

$$\sum_{l=1}^{3N_p} \left(\frac{\partial \mathbb{K}_{ij}}{\partial Y^l} \mathbb{K}_{lk} + \frac{\partial \mathbb{K}_{jk}}{\partial Y^l} \mathbb{K}_{li} + \frac{\partial \mathbb{K}_{ki}}{\partial Y^l} \mathbb{K}_{lj} \right). \quad (15)$$

Without loss of generality, we suppose that $\frac{\partial \mathbb{K}_{ij}}{\partial Y^l} \mathbb{K}_{lk} \neq 0$. When $k \in \{1, \dots, 3N_p\}$, it has $\mathbb{K}_{lk} = 0$. Thus, it only needs to focus on the case of $k \in \{3N_p + 1, \dots, 6N_p\}$.

Case 1. When $i, j \in \{1, \dots, 3N_p\}$, it has $\mathbb{K}_{ij} = 0$.

Case 2. When $i \in \{1, \dots, 3N_p\}, j \in \{3N_p + 1, \dots, 6N_p\}$, it has $\mathbb{K}_{li} = 0$. Then (15) becomes to

$$\sum_{l=1}^{3N_p} \left(\frac{\partial \mathbb{K}_{ij}}{\partial Y^l} \mathbb{K}_{lk} + \frac{\partial \mathbb{K}_{ki}}{\partial Y^l} \mathbb{K}_{lj} \right). \quad (16)$$

Since matrix \mathbb{N} and \mathbb{W}^{-1} are block diagonal, we only need to consider the case in which i, j, k, l are the subscripts for the same particle. According to $(D_F)_{ij} = \frac{\partial x_i}{\partial y_j}$ and the definition, it has $N_{ij} = \frac{\partial y_j}{\partial x_i}$. Since weighting matrix is constant and composed of the reciprocals of particles' weights. Thus, we can leave out them when verifying the identity, and term (16) turns into

$$\begin{aligned} & \frac{\partial}{\partial Y^l} \frac{\partial Y_i}{\partial X^j} \frac{\partial Y_l}{\partial X^k} - \frac{\partial}{\partial Y^l} \frac{\partial Y_i}{\partial X^k} \frac{\partial Y_l}{\partial X^j} \\ &= \frac{\partial^2 Y^i}{\partial X^k \partial X^j} - \frac{\partial^2 Y^i}{\partial X^j \partial X^k} \\ &= 0. \end{aligned}$$

If $j \in \{1, \dots, 3N_p\}, i \in \{3N_p + 1, \dots, 6N_p\}$, it is similar to this case and will not be repeated.

Case 3. When $i, j \in \{3N_p + 1, \dots, 6N_p\}$, it has $N_{ij}^T = \frac{\partial y_i}{\partial x_j}$ and

$$\hat{\mathbf{B}} = \mathbf{N} \hat{\mathbf{B}} \mathbf{N}^T,$$

Thus the following proof is similar to the case in [14].

Overall, if the magnetic field is divergence-free, Jacobi identity of bracket (9) is satisfied. □

4 Time discretization

In this section, we discuss time discretization methods for discrete systems (14). By noticing that it is not possible to solve the subsystem explicitly by using the splitting in [14] due to the matrix $N(y)$, the other structure-preserving methods should be applied. The charged-particle dynamic has been widely studied due to its significance for plasma physics [15, 16, 17]. In practical magnetic confinement devices, the external magnetic field is very strong (i.e. $0 < \varepsilon \ll 1$), which brings a new time scale (Larmor gyration) to single particle systems. When using classical numerical methods such as splitting algorithms, difference methods, etc. to simulate this problem, the dynamic behavior of charged particles can only be accurately characterized when the step size is less than the cyclotron period. And these calculations will be prohibitively expansive for long time simulation. Recently, a series of works [4, 19, 18] have been devoted to constructing numerical schemes to break the time step limit in Cartesian coordinate.

In order to simplify the notation, we will omit the indices in (8). Furthermore, we assume that $\mathbf{B}(x) = [0, 0, b(x)]^T$ (If $b(x) = b_0 + \varepsilon b_1(x)$, it is also called the maximal

ordering scaling). It also means $\hat{\mathbf{B}}(x) = b(x)K$ with $K = \begin{pmatrix} 0 & 1 & 0 \\ -1 & 0 & 0 \\ 0 & 0 & 0 \end{pmatrix}$. Then,

it follows that $\tilde{\mathbf{B}}(y) = [0, 0, J(y)b(x)]^T$ and $\hat{\tilde{\mathbf{B}}}(y) = J(y)b(F(y))K$. Certainly, it's no need to transfer x_3 due to our hypothesis for $\mathbf{B}(x)$ so that we suppose $y_1 = y_1(x_1, x_2), y_2 = y_2(x_1, x_2), y_3 = x_3$ in the rest part of this paper. We will use following notations for numerical analysis: $a_\alpha = [a_1, a_2]^T$ for $\forall a \in \mathbb{R}^3$, $A_\alpha = \begin{pmatrix} A_{11} & A_{12} \\ A_{21} & A_{22} \end{pmatrix}$ for $\forall A \in \mathbb{R}^{3 \times 3}$ and $S = K_\alpha$.

Then the charged-particle dynamic in orthogonal curvilinear coordinates can be expressed as

$$\begin{aligned} \varepsilon \dot{y} &= N^T(y)v, \\ \varepsilon \dot{v} &= N(y)\tilde{\mathbf{E}}(y) + \frac{b(F(y))}{\varepsilon}Kv, \\ y(0) &= y_0, \quad v(0) = v_0. \end{aligned} \tag{17}$$

In the limit $\varepsilon \rightarrow 0$, it follows that $y_\alpha \rightarrow u$, where u corresponds to the guiding center approximation¹

$$\begin{aligned} \dot{u} &= \text{sgn}(b(F(u)))(|b(F(u))|J(u))^{-1}S\tilde{\mathbf{E}}_\alpha(u) \\ &= (b(F(u))J(u))^{-1}S\tilde{\mathbf{E}}_\alpha(u) := \mathcal{R}(u), \quad u(0) = y_\alpha(0), \end{aligned} \tag{18}$$

where w.l.o.g we assume $b > 0$ (The magnetic field is used to confine the plasma, then this assumption is necessary).

4.1 Semi-implicit schemes

To solve system (17), we apply the implicit-explicit Runge-Kutta schemes developed in [32]. In this paper, we focus on the following two types.

APSI1: By denoting $\tau = \frac{\Delta t}{\varepsilon}$ and $\lambda = \frac{\Delta t}{\varepsilon^2}$, a first order semi-implicit scheme is given by

$$\begin{aligned} y^{n+1} &= y^n + \tau N(y^n)^T v^{n+1}, \\ v^{n+1} &= v^n + \tau N(y^n)\tilde{\mathbf{E}}(y^n) + \lambda b(F(y^n))Kv^{n+1}. \end{aligned} \tag{19}$$

(19) equals to

$$\begin{pmatrix} y^{n+1} \\ v^{n+1} \end{pmatrix} = \begin{pmatrix} I & -\tau N(y^n)^T \\ 0 & I - \lambda b(F(y^n))K \end{pmatrix}^{-1} \begin{pmatrix} y^n \\ v^n + \tau N(y^n)\tilde{\mathbf{E}}(y^n) \end{pmatrix}.$$

For the upper triangular matrix above, its inverse matrix is easy to calculate according to covariant basis and skew-symmetric matrix K . Specifically, it is

$$\begin{pmatrix} I & \tau N(y^n)^T + \frac{\tau \lambda b(F(y^n))}{1+(\lambda b(F(y^n)))^2} N(y^n)^T K + \frac{\tau \lambda^2 b(F(y^n))^2}{1+(\lambda b(F(y^n)))^2} N(y^n)^T K^2 \\ 0 & I + \frac{\lambda b(F(y^n))}{1+(\lambda b(F(y^n)))^2} K + \frac{\lambda^2 b(F(y^n))^2}{1+(\lambda b(F(y^n)))^2} K^2 \end{pmatrix}.$$

¹The results are corresponding to conclusions of Cartesian coordinate in [26, 11, 6, 10].

APSI2: Moreover, a second order L-stable scheme can be written as

$$\begin{aligned}
y_n^{(1)} &= y^n + \gamma\tau N(y^n)^T v_n^{(1)}, \\
v_n^{(1)} &= v^n + \gamma\tau F_n^{(1)}, \\
y^{n+1} &= y^n + (1-\gamma)\tau N(y^n)^T v_n^{(1)} + \gamma\tau N(y^n)^T v^{n+1}, \\
v^{n+1} &= v^n + (1-\gamma)\tau F_n^{(1)} + \gamma\tau F_n^{(2)}.
\end{aligned} \tag{20}$$

where $\gamma = 1 - 1/\sqrt{2}$ and

$$\begin{aligned}
y_n^{(2)} &= y^n + \frac{\tau}{2\gamma} N(y^n)^T v_n^{(1)}, \\
F_n^{(1)} &= N(y^n) \tilde{\mathbf{E}}(y^n) + \frac{b(F(y^n))}{\varepsilon} K v_n^{(1)}, \\
F_n^{(2)} &= N(y_n^{(2)}) \tilde{\mathbf{E}}(y_n^{(2)}) + \frac{b(F(y_n^{(2)}))}{\varepsilon} K v^{n+1}.
\end{aligned}$$

For a vector form, it reads

$$\begin{aligned}
\begin{pmatrix} y_n^{(1)} \\ v_n^{(1)} \end{pmatrix} &= \begin{pmatrix} I & -\gamma\tau N(y^n)^T \\ 0 & I - \gamma\lambda b(F(y^n))K \end{pmatrix}^{-1} \begin{pmatrix} y^n \\ v^n + \gamma\tau N(y^n) \tilde{\mathbf{E}}(y^n) \end{pmatrix}, \\
\begin{pmatrix} y^{n+1} \\ v^{n+1} \end{pmatrix} &= \begin{pmatrix} I & -\gamma\tau N(y_n^{(2)})^T \\ 0 & I - \gamma\lambda b(F(y_n^{(2)}))K \end{pmatrix}^{-1} \begin{pmatrix} y^n + (1-\gamma)\tau N(y^n)^T v_n^{(1)} \\ v^n + (1-\gamma)\tau F_n^{(1)} + \gamma\tau N(y_n^{(2)}) \tilde{\mathbf{E}}(y_n^{(2)}) \end{pmatrix}.
\end{aligned}$$

4.2 Uniform estimate

Then we focus on the asymptotic-preserving property of these algorithms. For convenience, we will ignore subscripts α in the proof and use b^n to denote $b(F(y^n))$. As a result, we have the following theorem for scheme (19).

Theorem 4.1. *Assume that $\mathbf{E} \in W^{1,\infty}$, $\tilde{\Omega}_y$ and Ω_x are compact. Then for the solution (y^n, v^n) to equation (19) in a finite time T , there exists constants C and λ_0 such that when $\lambda \geq \lambda_0$ the following estimate holds*

$$\|y^n - u^n\| \leq C\varepsilon^2 \left(1 + \|\varepsilon^{-1}v^0 - (b^0)^{-1}SN(y^0)\tilde{\mathbf{E}}(y^0)\| \right) \tag{21}$$

where u^n is the numerical solution of the following guiding-center model

$$u^{n+1} = u^n + \Delta t \mathcal{R}(u^n), \quad u^0 = y^0. \tag{22}$$

Proof. Since $\mathbf{E} \in W^{1,\infty}$, $\tilde{\Omega}_y$ and Ω_x are compact, electric field, inverse Jacobi matrix, Jacobian with its reciprocal and first-order derivative are all bounded. So a common upper bound κ is taken for estimates. Firstly we introducing intermediate variables

$$z^n = \varepsilon^{-1}v^n - (b^{n-1})^{-1}SN(y^{n-1})\tilde{\mathbf{E}}(y^{n-1}). \tag{23}$$

On the other hand, we have

$$v^1 = (I - \lambda b^0 S)^{-1} (v^0 + \tau N(y^0) \tilde{\mathbf{E}}(y^0)).$$

Since $(I - \beta S)^{-1} = \frac{I + \beta S}{1 + \beta^2}$ holds for $\forall \beta \in \mathbb{R}$, it yields that

$$z^1 = \frac{I + \lambda b^0 S}{1 + (\lambda b^0)^2} \left(\varepsilon^{-1} v^0 - (b^0)^{-1} S N(y^0) \tilde{\mathbf{E}}(y^0) \right).$$

And the following equality holds according to (23)

$$z^{n+1} = \frac{I + \lambda b^n S}{1 + (\lambda b^n)^2} \left(z^n - S \left((b^n)^{-1} N(y^n) \tilde{\mathbf{E}}(y^n) - (b^{n-1})^{-1} N(y^{n-1}) \tilde{\mathbf{E}}(y^{n-1}) \right) \right) \quad (24)$$

for $\forall n \geq 1$. Due to (19), it has

$$y^n = y^{n-1} + \tau N(y^{n-1})^T v^n = y^{n-1} + \Delta t N(y^{n-1})^T z^n + \Delta t \mathcal{R}(y^{n-1}). \quad (25)$$

Let $\Lambda = \left\| \frac{1 + \lambda b(F(y))}{1 + (\lambda b(F(y)))^2} \right\|_{\infty}$, $a := \Lambda \max \{1 + 2\kappa^2 \Delta t, 1 + 2\kappa^3 \Delta t\}$, $b := 2\Lambda \kappa^4 \Delta t$ and $c := \Lambda \|\varepsilon^{-1} v^0 - (b^0)^{-1} S N(y^0) \tilde{\mathbf{E}}(y^0)\|$. By fixing the time step Δt , when $\varepsilon \rightarrow 0$, it has $\lambda \rightarrow \infty$. Thus there exists constants $\lambda_0, \alpha > 0$ such that $a \leq \alpha < 1$ when $\lambda \geq \lambda_0$. After taking the norm on (24)'s both sides, it yields $\|z^{n+1}\| \leq a^n c + \frac{b}{1-a}$. By taking the difference as $e^n := y^n - u^n$, it can be obtained that

$$\|e^n\| \leq \frac{a}{\Lambda} \|e^{n-1}\| + \kappa \Delta t a^{n-1} c + \kappa \Delta t \frac{b}{1-a}.$$

Finally, (21) holds due to $e^0 = 0$. □

On the other hand, one can get a better result if the initial value in (22) is modified.

Corollary 1. *If the conditions in theorem (4.1) hold, it has the following estimate:*

$$\|y^n - u^n\| \leq C \varepsilon^2 \left(1 + \left(\frac{1}{\lambda} + \Delta t \right) \|\varepsilon^{-1} v^0 - (b^0)^{-1} S N(y^0) \tilde{\mathbf{E}}(y^0)\| \right),$$

where u^n is the numerical solution of equation (22) with modified initial value

$$u^0 = y^0 + \frac{\varepsilon}{b^0} N(y^0)^T \left(S v^0 + \frac{\varepsilon}{b^0} N(y^0) \tilde{\mathbf{E}}(y^0) \right).$$

Proof. By noting that

$$z^1 = \left(\frac{S}{\lambda b^0} + \frac{\lambda b^0 I - S}{\lambda b^0 (1 + (\lambda b^0)^2)} \right) \left(\varepsilon^{-1} v^0 - (b^0)^{-1} S N(y^0) \tilde{\mathbf{E}}(y^0) \right),$$

and then it has

$$e^1 = \Delta t \mathcal{R}(y^0) - \Delta t \mathcal{R}(u^0) + \Delta t N(y^0)^T \frac{\lambda b^0 I - S}{\lambda b^0 (1 + (\lambda b^0)^2)} \left(\varepsilon^{-1} v^0 - (b^0)^{-1} S N(y^0) \tilde{\mathbf{E}}(y^0) \right).$$

Moreover, it follows that

$$\begin{aligned} \|e^n\| &\leq \left(\frac{a}{\Lambda} \right)^{n-1} \|e^1\| + C(\kappa) \frac{\Delta t}{\lambda} a^{n-1} c \left(\left(\frac{1}{\Lambda} \right)^{n-1} - 1 \right) + C(T, \kappa) \frac{b}{1-a}, \\ &\leq C(T, \kappa, \alpha, b_0) \varepsilon^2 \left(\Delta t + \frac{1}{\lambda} \right) \|\varepsilon^{-1} v^0 - (b^0)^{-1} S N(y^0) \tilde{\mathbf{E}}(y^0)\| + C(T, \kappa) \varepsilon^2. \end{aligned}$$

□

For scheme (20), it follows:

Theorem 4.2. *Under the assumptions of theorem (4.1), the estimate (21) holds for (y^n, v^n) to equation (20) while u^n is the numerical solution of the guiding-center model*

$$u^{n+1} = u^n + (1-\gamma)\Delta t \mathcal{R}(u^n) + \gamma \Delta t \mathcal{R}(u^{(1)}), \quad u^{(1)} = u^n + \frac{\Delta t}{2\gamma} \mathcal{R}(u^n), \quad u^0 = y^0. \quad (26)$$

Proof. The proof is similar to Theorem 4.1, we briefly present the key points. By using $\mathcal{F}(y) = D_F(y)\mathcal{R}(y)$, we can define

$$z_1^n = \varepsilon^{-1}v_n^{(1)} - \mathcal{F}(y^{n-1}), \quad z_2^n = \varepsilon^{-1}v_n - \mathcal{F}(y_{n-1}^{(2)}).$$

Then due to scheme (20), it follows that

$$\begin{aligned} z_1^{n+1} &= (I - \gamma \lambda b^n S)^{-1} (z_2^n + \mathcal{F}(y_{n-1}^{(2)}) - \mathcal{F}(y_n)), \\ z_2^{n+1} &= \left(I - \gamma \lambda b(F(y_n^{(2)})) S \right)^{-1} (z_2^n + \mathcal{F}(y_{n-1}^{(2)})) - \mathcal{F}(y_n^{(2)}) + (1 - \gamma) \lambda b^n S z_1^{n+1}. \end{aligned}$$

By denoting $\Lambda = \left\| \frac{1 + \lambda \gamma b(F(y))}{1 + (\lambda \gamma b(F(y)))^2} \right\|_\infty$, it has

$$\begin{aligned} \|z_1^{n+1}\| &\leq C(\kappa) \Lambda (\|z_2^n\| + \Delta t \|z_1^n\| + \Delta t(1 + \gamma)), \\ \|z_2^{n+1}\| &\leq C(\kappa) \Lambda \left(\left(\frac{\Delta t}{2\gamma} + (1 - \gamma)\lambda \right) \|z_1^{n+1}\| + \Delta t \|z_1^n\| + \|z_2^n\| + \Delta t \right), \end{aligned} \quad (27)$$

due to

$$\begin{aligned} \|y_{n-1}^{(2)} - y^n\| &\leq C(\kappa) \tau \|v_{n-1}^{(1)} - \gamma v^n\| \leq C(\kappa) \Delta t (\|z_1^n\| + \|z_2^n\| + (1 + \gamma)), \\ \|y_{n-1}^{(2)} - y_n^{(2)}\| &\leq C(\kappa) \Delta t \left(\frac{1}{2\gamma} \|z_1^{n+1}\| + \|z_1^n\| + \gamma \|z_2^n\| + 1 \right). \end{aligned}$$

Then (27) leads to

$$\|z_1^{n+1}\| + \|z_2^{n+1}\| \leq C(\kappa) \Lambda (\|z_1^n\| + \|z_2^n\| + \Delta t).$$

On the other hand, by taking difference between y^{n+1} and u^{n+1} , (21) holds due to

$$\|e^{n+1}\| \leq C(\kappa) (\|e^n\| + \Delta t \|z_1^{n+1}\| + \Delta t \|z_2^{n+1}\|)$$

and

$$\begin{aligned} z_1^1 &= \frac{I + \gamma \lambda b^0 S}{1 + (\gamma \lambda b^0)^2} \left(\varepsilon^{-1} v^0 - (b^0)^{-1} S N(y^0) \tilde{E}(y^0) \right), \\ z_2^1 &= \frac{I + \gamma \lambda b(F(y_0^{(2)})) S}{1 + (\gamma \lambda b(F(y_0^{(2)}))^2} \left(\varepsilon^{-1} v^0 + (1 - \gamma) \lambda b^0 z_1^1 - \mathcal{F}(y_0^{(2)}) \right). \end{aligned}$$

□

5 Numerical experiment

In this section, we display some examples to verify the analysis results. By simulating the motion of a single particle, the asymptotic-preserving properties of schemes can be observed and compare to our theoretical results. Then an application of a 2 + 2-dimensional Vlasov system is presented to display the advantage of our algorithm. Last but not least, we consider the cylindrical coordinate transformation

$$x_1 = r \cos(\theta), \quad x_2 = r \sin(\theta), \quad x_3 = z,$$

for $y = (r, \theta, z)$.

5.1 Benchmark problem

First, a benchmark numerical test is carried out to show the efficiency of our proposed algorithms and verify the uniform estimate of them. We consider the electromagnetic field with $\mathbf{E}(x) = -x$, $b(x) = 1 + \varepsilon \sin(\sqrt{x_1^2 + x_2^2})$, and the initial data $y(0) = (0.36, 0.6, -1.4)^T$, $v(0) = (-0.7, 0.08, 0.2)^T$.

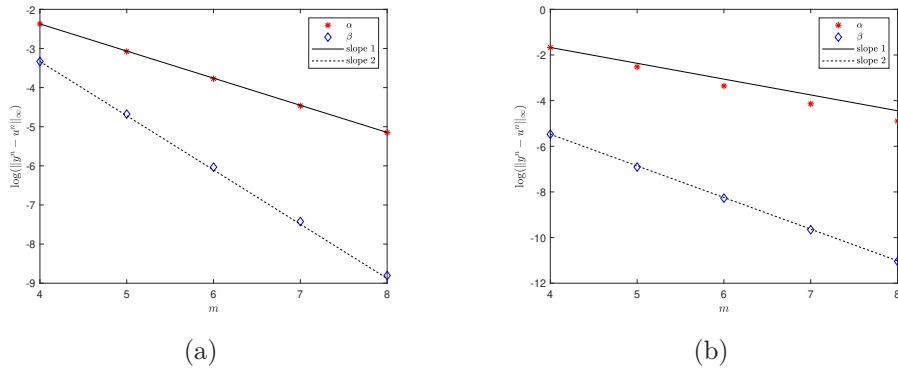


Figure 1: Uniform estimates of schemes with time step $\Delta t = 0.1$ for $\varepsilon = 2^{-m}$ and $T = 10$. α : Original initial data. β : Modified initial data $v^0 = \varepsilon(b^0)^{-1}SN(y^0)\tilde{\mathbf{E}}(y^0)$. (a): APSI1 (19). (b): APSI2 (20).

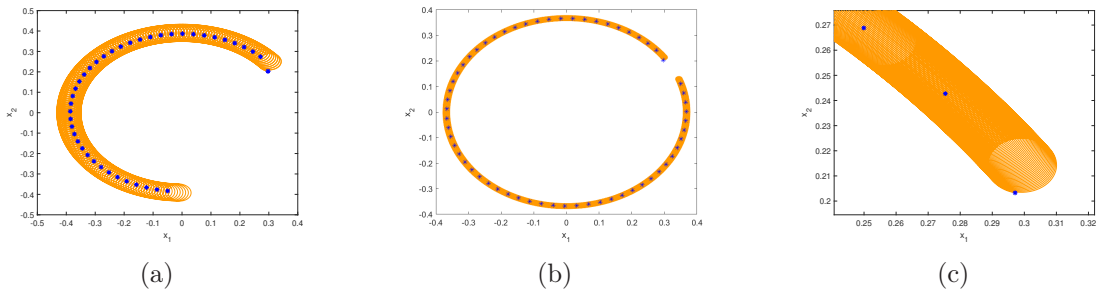


Figure 2: Comparison between a reference solution (Boris method with time step ε^2) and the solution of algorithm (19) with time step $\Delta t = 0.1$. (a): $\varepsilon = 2^{-4}$, $T = 1/\sqrt{\varepsilon}$. (b): $\varepsilon = 2^{-6}$, $T = 0.75/\sqrt{\varepsilon}$. (c): A zoom of the left part.

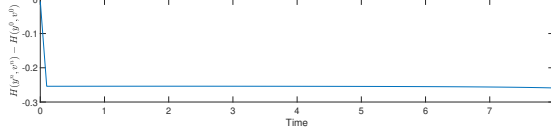


Figure 3: Time evolutions of error of energy with time step $\Delta t = 0.1$ for $\varepsilon = 2^{-8}$ and $T = 0.5/\sqrt{\varepsilon}$. Here, $\mathbf{E}(x) = -\nabla\phi(x)$ with $\phi = 1/3(x_1^3 + x_2^3)$.

In Figure 1, it can be observed that numerical errors match our theoretical estimations well (by noticing $\|\varepsilon^{-1}v^0 - (b^0)^{-1}SN(y^0)\tilde{\mathbf{E}}(y^0)\| = \mathcal{O}(\varepsilon^{-1})$). Since numerical results of two algorithms in Figure 2 and Figure 3 are nearly the same, so we just plot one of them. And they show our method is able to capture the high oscillations of the solution even with a very coarse time step and preserve the energy well over long time.

5.2 Diocotron instability

In this experiment, the magnetic field $\mathbf{B} = (0, 0, 1)^T$ is uniform and initial distribution function is taken as

$$f_0(y, v) = \frac{d_0(y)}{2\pi} \exp\left(-\frac{|v|^2}{2}\right), \quad y = (r, \theta) \in \mathbb{R}_+ \times \mathbb{R},$$

where the initial density is

$$d_0(\mathbf{x}) = \begin{cases} (1 + \alpha \cos(l\theta)) \exp(-4(r - 6.5)^2) & \text{if } r^- \leq r \leq r^+, \\ 0 & \text{otherwise,} \end{cases}$$

with l the number of vortices. In our simulation, we take $r^- = 5, r^+ = 8, \alpha = 0.2$. The parameter ε is used to control the strength of the magnetic field. We consider the particle equations on the orthogonal planes to magnetic field after transformation, that is

$$\varepsilon \dot{y} = N^T v,$$

$$\varepsilon \dot{v} = N \tilde{\mathbf{E}}_h + \frac{1}{\varepsilon} S v,$$

$$\tilde{\mathbf{E}}_h = \nabla_y \tilde{\phi}_h,$$

$$\int_{\tilde{\Omega}_y} \left(r \frac{\partial \tilde{\phi}_h}{\partial r} \frac{\partial \psi}{\partial r} + \frac{1}{r} \frac{\partial \tilde{\phi}_h}{\partial \theta} \frac{\partial \psi}{\partial \theta} \right) dy = \int_{\tilde{\Omega}_y} \psi \sum_{s=1}^{N_p} \alpha_s \zeta_r(y - Y_s(t)) dy, \quad \forall \psi \in H_0^1(\tilde{\Omega}_y).$$

where $N = \begin{pmatrix} \cos \theta & -\frac{\sin \theta}{r} \\ \sin \theta & \frac{\cos \theta}{r} \end{pmatrix}$, and ζ_r is a regularizing function for Dirac function.

Now, we can reduce the size of the calculation to simulate the same thing. Specifically, we choose $(x_1, x_2) \in [-4\pi, 4\pi] \times [-4\pi, 4\pi]$ in [14] and $(r, \theta) \in [2, 4\pi] \times [0, 2\pi]$ for now. Uniform grid of r - θ plane also equals to divide the computational domain on a ring in x - y plane by the approach showed in Figure 4. Moreover, Figure 5 and 6 show the results of our calculations when we take the parameters $\varepsilon = 0.1$ and $\varepsilon = 0.01$, respectively, and the step size is chosen as $\Delta t = 0.1$. The

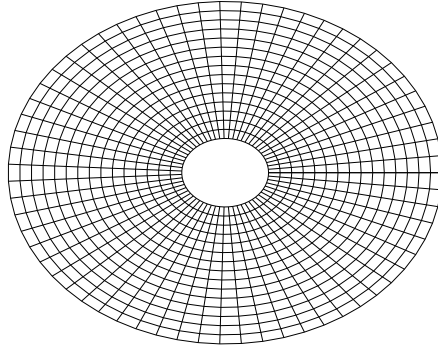


Figure 4: Grid of the computational domain.

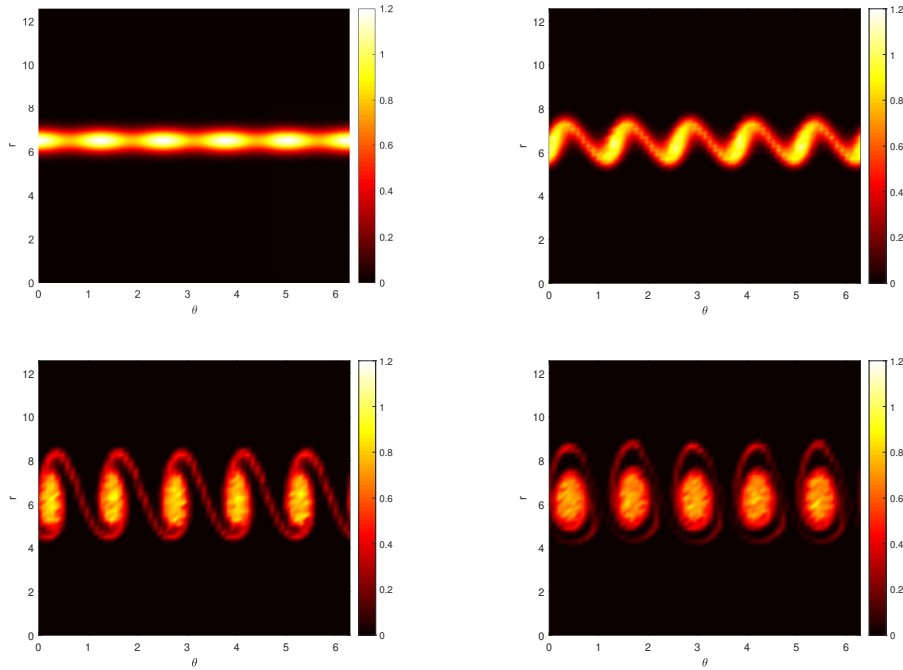


Figure 5: Time evolution of the density ρ for time $t = 0, 10, 20, 30$ and $l = 5$ with parameter $\varepsilon = 0.1$.

finite element mesh parameters are $N_r = N_\theta = 64$ and $N_r = N_\theta = 128$ respectively. Moreover, the number of particles is more than 10^6 , and for the variable θ we assume the periodic boundary condition. Despite our low resolution, the instability phenomenon is still captured well. They are also consistent with our results in Cartesian coordinates in [14]. At the same time, it can also be seen that the use of cylindrical coordinate makes it easier to observe the confining effect of the magnetic field on the plasma, and we can try to further reduce the computational area.

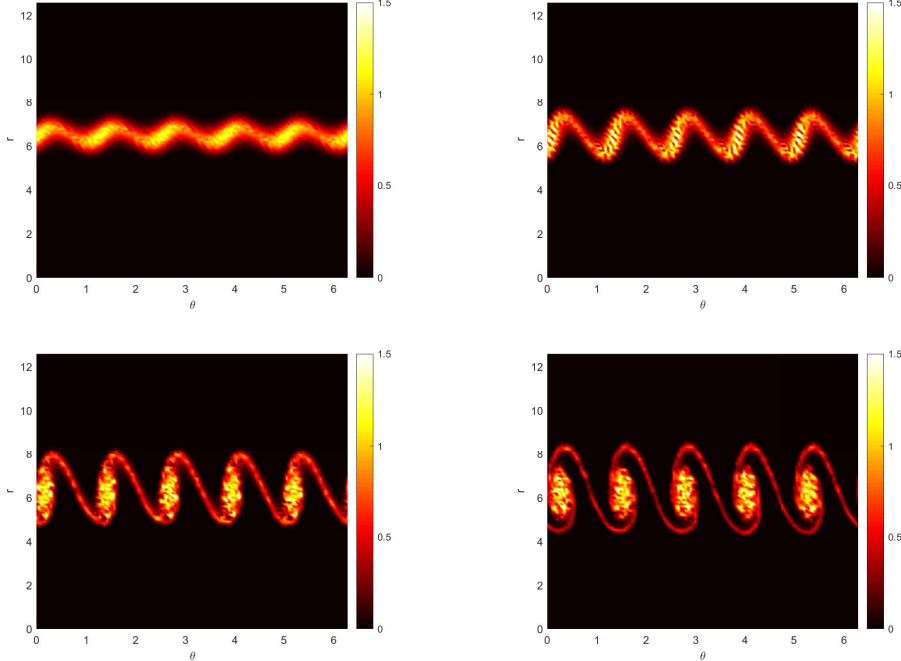


Figure 6: Time evolution of the density ρ for time $t = 5, 10, 15, 20$ and $l = 5$ with parameter $\varepsilon = 0.01$.

6 Conclusion

In this work, we have developed the Particle-in-Cell methods for solving the magnetized Vlasov–Poisson system in orthogonal curvilinear coordinates. For numerical algorithms construction, we use the finite element method in space and the semi-implicit method in time. Also, asymptotic preservation property of the full discretization method is verified, and it guarantees the numerical simulation over long-time. We present a $2 + 2$ -dimensional example for application, in this case the external magnetic field can be strong. It can be found that the algorithm can accurately portray the physical phenomena, reflecting the constraint effect of the magnetic field on the plasma. The use of appropriate curve coordinates for numerical experiments also saves computational resources.

After spatial discretization in curvilinear coordinates we get discrete Hamiltonian systems. However, semi-implicit algorithms, although asymptotically stable, generally do not preserve the discrete Poisson structure, and we will try to find more temporal methods that can preserve the geometric structure and are easy to implement. In addition, we consider the strong magnetic field with one direction due to the two-dimensional guiding center approximation. To extend the algorithms and analysis for a general case is the next work.

A Vector fields in orthogonal curvilinear coordinates

We assume that $x = (x_1, x_2, x_3)$ is Cartesian coordinate and $y = (y_1, y_2, y_3)$ is an orthogonal coordinate. Then we have

$$dx_i = \sum_j \frac{\partial x_i}{\partial y_j} dy_j.$$

Further, the quadratic form

$$ds^2 = \sum_i dx_i^2$$

has the following form in curvilinear coordinate

$$ds^2 = \sum_{ij} g_{ij} dy_i dy_j,$$

where

$$g_{ij} = t_i \cdot t_j$$

and

$$t_i = \frac{\partial x}{\partial y_i}$$

is called covariant basis. At the same time, there exist dual contravariant basis n_1, n_2, n_3 satisfying $t_i \cdot n_j = \delta_{ij}$. And since the coordinate system is orthogonal we have

$$g_{ij} = \begin{cases} g_{ii}, & i = j, \\ 0, & i \neq j. \end{cases}$$

Denote the positive numbers $H_i = \sqrt{g_{ii}}$ and they are often called Lamé coefficients. If the corresponding map on the domain is a diffeomorphism, its tangent map is an isomorphism. That is, the standard orthogonal basis of Cartesian coordinate corresponds to a set of covariant basis in curvilinear coordinate, but in general the latter are not unit vectors, and the moduli of these basis vectors are Lamé coefficient H_i s. Therefore the unit basis vectors in the curvilinear coordinate will be

$$e_i = \frac{1}{H_i} \frac{\partial x}{\partial y_i} = \frac{1}{H_i} t_i.$$

On the other hand, with these coefficients, we can consider the differential forms of the curvilinear coordinate. The volume element can be expressed as

$$dV = H_1 H_2 H_3 dy_1 dy_2 dy_3.$$

For a scalar field f , the gradient is

$$\text{grad} f = \nabla f = \sum_i \frac{1}{H_i} \frac{\partial f}{\partial y_i} e_i.$$

By using bases, the gradient operator can also be expressed as $\nabla = \sum_i \frac{\partial}{\partial y_i} n_i$.

For a vector field B , the divergence is

$$\operatorname{div} B = \nabla \cdot B = \frac{1}{H_1 H_2 H_3} \sum_i \frac{\partial}{\partial y_i} (H_j H_k B_i).$$

For a scalar field f , the Laplace operator is

$$\Delta f = \operatorname{div}(\operatorname{grad} f) = \frac{1}{H_1 H_2 H_3} \sum_i \frac{\partial}{\partial y_i} \left(\frac{H_j H_k}{H_i} \frac{\partial f}{\partial y_i} \right),$$

where $i, j, k \in \{1, 2, 3\}$ and are different from each other.

Example A.1. *Cylindrical coordinate*

We consider the cylindrical coordinate

$$(r, \theta, z)$$

with the mapping

$$x = r \cos \theta, \quad y = r \sin \theta, \quad z.$$

By defining covariant basis as

$$\begin{aligned} t_1 &= \frac{\partial(xe_1 + ye_2 + ze_3)}{\partial r} = \cos \theta e_1 + \sin \theta e_2 = e_r, \\ t_2 &= \frac{\partial(xe_1 + ye_2 + ze_3)}{\partial \theta} = -r \sin \theta e_1 + r \cos \theta e_2 = r e_\theta, \\ t_3 &= \frac{\partial(xe_1 + ye_2 + ze_3)}{\partial z} = e_3 = e_z, \end{aligned}$$

it is straightforward to derive the contravariant basis as

$$n_1 = e_r, \quad n_2 = \frac{1}{r} e_\theta, \quad n_3 = e_z,$$

The Lamé coefficients are obtained from covariant basis as

$$H_1 = 1, \quad H_2 = r, \quad H_3 = 1,$$

Then the quadratic form is

$$ds^2 = dr^2 + r^2 d\theta^2 + dz^2,$$

the volume element is

$$dV = r dr d\theta dz,$$

the gradient, divergence and Laplace operator are

$$\begin{aligned} \operatorname{grad} f &= \nabla f = \frac{\partial f}{\partial r} e_r + \frac{1}{r} \frac{\partial f}{\partial \theta} e_\theta + \frac{\partial f}{\partial z} e_z, \\ \operatorname{div} B &= \frac{1}{r} \left(\frac{\partial(rB_r)}{\partial r} + \frac{\partial B_\theta}{\partial \theta} + \frac{\partial(rB_z)}{\partial z} \right), \\ \Delta f &= \frac{1}{r} \left(\frac{\partial}{\partial r} \left(r \frac{\partial f}{\partial r} \right) + \frac{\partial}{\partial \theta} \left(\frac{1}{r} \frac{\partial f}{\partial \theta} \right) + \frac{\partial}{\partial z} \left(r \frac{\partial f}{\partial z} \right) \right). \end{aligned}$$

B Propositions

Proposition B.1. [31] $K(x)$ is the structure matrix for a Poisson bracket if and only if it has the following properties:

(1) Skew-symmetry:

$$K_{ij}(x) = -K_{ji}(x), \quad i, j = 1, \dots, m,$$

(2) Jacobi identity:

$$\sum_{l=1}^m \left(\frac{\partial K_{ij}}{\partial x_l} K_{lk} + \frac{\partial K_{jk}}{\partial x_l} K_{li} + \frac{\partial K_{ki}}{\partial x_l} K_{lj} \right) = 0.$$

Proposition B.2. The matrix

$$\hat{\mathbf{B}} = \begin{pmatrix} 0 & \mathbf{B}_3 & -\mathbf{B}_2 \\ -\mathbf{B}_3 & 0 & \mathbf{B}_1 \\ \mathbf{B}_2 & -\mathbf{B}_1 & 0 \end{pmatrix}$$

with respect to the magnetic field \mathbf{B} satisfies

$$\hat{\mathbf{B}}^3 = -b^2 \hat{\mathbf{B}}, \quad (\mathbf{B} \cdot y) \mathbf{B} = \hat{\mathbf{B}}^2 y + b^2 y,$$

$|\mathbf{B}| = b$ and it holds for any vector $y \in \mathbb{R}^3$.

References

- [1] C. K. Birdsall and A. B. Langdon. *Plasma Physics Via Computer Simulation*. CRC Press, 1991.
- [2] Fernando Casas, Nicolas Crouseilles, Erwan Faou, and Michel Mehrenberger. High-order Hamiltonian splitting for Vlasov–Poisson equations. *Numerische Mathematik*, 135(3):769–801, 2017.
- [3] L. Chacón and G. Chen. A curvilinear, fully implicit, conservative electro-magnetic PIC algorithm in multiple dimensions. *Journal of Computational Physics*, 316:578–597, 2016.
- [4] Philippe Chartier, Nicolas Crouseilles, Mohammed Lemou, Florian Méhats, and Xiaofei Zhao. Uniformly Accurate Methods for Three Dimensional Vlasov Equations under Strong Magnetic Field with Varying Direction. *SIAM Journal on Scientific Computing*, 42(2):B520–B547, 2020.
- [5] Nicolas Crouseilles, Lukas Einkemmer, and Erwan Faou. Hamiltonian splitting for the Vlasov–Maxwell equations. *Journal of Computational Physics*, 283:224–240, 2015.
- [6] Pierre Degond and Francis Filbet. On the asymptotic limit of the three dimensional Vlasov–Poisson system for large magnetic field: Formal derivation. *Journal of Statistical Physics*, 165:765–784, 2016.
- [7] E. G. Evstatiev and B. A. Shadwick. Variational formulation of particle algorithms for kinetic plasma simulations. *Journal of Computational Physics*, 245:376–398, 2013.

- [8] Kang Feng. Proceedings of the 1984 Beijing Symposium of Differential Geometry and Differential Equations—Computation of Partial Differential Equation. *Science Press, Beijing*, page 42–58, 1985.
- [9] Kang Feng and Mengzhao Qin. *Symplectic Geometric Algorithms for Hamiltonian Systems*. Springer, Berlin, Heidelberg, 2010.
- [10] Francis Filbet and L. Miguel Rodrigues. Asymptotics of the three-dimensional Vlasov equation in the large magnetic field limit. *Journal de l'École polytechnique — Mathématiques*, 7:1009–1067, 2020.
- [11] Francis Filbet and Luis Miguel Rodrigues. Asymptotically stable Particle-in-Cell methods for the Vlasov–Poisson system with a strong external magnetic field. *SIAM Journal on Numerical Analysis*, 54(2):1120–1146, 2016.
- [12] Francis Filbet and Luis Miguel Rodrigues. Asymptotically preserving particle methods for strongly magnetized plasmas in a torus. *Journal of Computational Physics*, 480:112015, 2023.
- [13] Francis Filbet and Eric Sonnendrücker. Numerical methods for the Vlasov equation. In *Numerical Mathematics and Advanced Applications*, pages 459–468, Milano, 2003. Springer Milan.
- [14] A. Gu, Y. He, and Y. Sun. Hamiltonian Particle-in-Cell methods for Vlasov–Poisson equations. *Journal of Computational Physics*, 467:111472, 2022.
- [15] Ernst Hairer and Christian Lubich. Symmetric multistep methods for charged-particle dynamics. *The SMAI Journal of computational mathematics*, 3:205–218, 2017.
- [16] Ernst Hairer and Christian Lubich. Energy behaviour of the boris method for charged-particle dynamics. *BIT Numerical Mathematics*, 58:969–979, 2018.
- [17] Ernst Hairer and Christian Lubich. Long-term analysis of a variational integrator for charged-particle dynamics in a strong magnetic field. *Numerische Mathematik*, 144:699–728, 2020.
- [18] Ernst Hairer, Christian Lubich, and Yanyan Shi. Large-stepsize integrators for charged-particle dynamics over multiple time scales. *Numerische Mathematik*, 151:659–691, 2022.
- [19] Ernst Hairer, Christian Lubich, and Bin Wang. A filtered boris algorithm for charged-particle dynamics in a strong magnetic field. *Numerische Mathematik*, 144:787–809, 2020.
- [20] Adnane Hamiaz, Michel Mehrenberger, Hocine Sellama, and Eric Sonnendrücker. The semi-Lagrangian method on curvilinear grids. *Communications in Applied and Industrial Mathematics*, 7(3):99–137, 2016.
- [21] Yang He, Yajuan Sun, Hong Qin, and Jian Liu. Hamiltonian particle-in-cell methods for Vlasov–Maxwell equations. *Physics of Plasmas*, 23(9):092108, 2016.
- [22] R. W. Hockney and J. W. Eastwood. *Computer Simulation Using Particles*. Institute of Physics Publishing, Bristol, 1988.
- [23] Michael Kraus, Katharina Kormann, Philip J. Morrison, and Eric Sonnendrücker. GEMPIC: Geometric electromagnetic particle-in-cell methods. *Journal of Plasma Physics*, 83(4):905830401, 2017.

- [24] Yingzhe Li, Yang He, Yajuan Sun, Jitse Niesen, Hong Qin, and Jian Liu. Solving the Vlasov–Maxwell equations using Hamiltonian splitting. *Journal of Computational Physics*, 396:381–399, 2019.
- [25] Jerrold E. Marsden and Alan Weinstein. The Hamiltonian structure of the Maxwell–Vlasov equations. *Physica D: Nonlinear Phenomena*, 4(3):394–406, 1982.
- [26] J. D. Meiss and R. D. Hazeltine. Canonical coordinates for guiding center particles. *Physics of Fluids B: Plasma Physics*, 2(11):2563–2567, 1990.
- [27] P. J. Morrison. A general theory for gauge-free lifting. *Physics of Plasmas*, 20(1):012104, 2013.
- [28] Philip J. Morrison. The Maxwell–Vlasov equations as a continuous Hamiltonian system. *Physics Letters A*, 80(5):383–386, 1980.
- [29] Philip J. Morrison. Hamiltonian description of the ideal fluid. *Review of Modern Physics*, 70:467–521, Apr 1998.
- [30] Philip J. Morrison. Structure and structure-preserving algorithms for plasma physics. *Physics of Plasmas*, 24:055502, 2017.
- [31] Peter J. Olver. *Applications of Lie Groups to Differential Equations*. Graduate Texts in Mathematics. Springer, New York, 1986.
- [32] Lorenzo Pareschi and Giovanni Russo. Implicit-explicit Runge-Kutta schemes and applications to hyperbolic systems with relaxation. *Journal of Scientific Computing*, 25:129–155, 2005.
- [33] Benedikt Perse, Katharina Kormann, and Eric Sonnendrücker. Geometric Particle-in-Cell Simulations of the Vlasov–Maxwell System in Curvilinear Coordinates. *SIAM Journal on Scientific Computing*, 43(1):B194–B218, 2021.
- [34] Benedikt Perse, Katharina Kormann, and Eric Sonnendrücker. Geometric Particle-in-Cell Simulations of the Vlasov–Maxwell System in Curvilinear Coordinates. *SIAM Journal on Scientific Computing*, 43(1):B194–B218, 2021.
- [35] Benedikt Perse, Katharina Kormann, and Eric Sonnendrücker. Perfect Conductor Boundary Conditions for Geometric Particle-in-Cell Simulations of the Vlasov–Maxwell System in Curvilinear Coordinates. *arXiv preprint arXiv:2111.08342*, 2021.
- [36] Martin Campos Pinto, Katharina Kormann, and Eric Sonnendrücker. Variational Framework for Structure-Preserving Electromagnetic Particle-In-Cell Methods. *arXiv preprint arXiv:2101.09247*, 2021.
- [37] Hong Qin, Jian Liu, Jianyuan Xiao, Ruili Zhang, Yang He, Yulei Wang, Yajuan Sun, Joshua W. Burby, Leland Ellison, and Yao Zhou. Canonical symplectic particle-in-cell method for long-term large-scale simulations of the Vlasov–Maxwell equations. *Nuclear Fusion*, 56(1):014001, 2016.
- [38] Jonathan Squire, Hong Qin, and William M. Tang. Geometric integration of the Vlasov–Maxwell system with a variational particle-in-cell scheme. *Physics of Plasmas*, 19(08):084501, 2012.
- [39] Jianyuan Xiao, Hong Qin, and Jian Liu. Structure-preserving geometric particle-in-cell methods for Vlasov–Maxwell systems. *Plasma Science and Technology*, 20(11):110501, sep 2018.

- [40] Jianyuan Xiao, Hong Qin, Jian Liu, Yang He, Ruili Zhang, and Yajuan Sun. Explicit high-order non-canonical symplectic particle-in-cell algorithms for Vlasov–Maxwell systems. *Physics of Plasmas*, 22:112504, 2015.